Acta Astronautica 112 (2015) 158–165

Contents lists available at ScienceDirect

Acta Astronautica

journal homepage: www.elsevier.com/locate/actaastro

An overnight habitat for expanding lunar surface exploration

Samuel S. Schreiner [a,*], Timothy P. Setterfield [a], Daniel R. Roberson [a], Benjamin Putbrese [a], Kyle Kotowick [a], Morris D. Vanegas [a], Mike Curry [a], Lynn M. Geiger [a], David Barmore [a], Jordan J. Foley [a], Paul A. LaTour [a], Jeffrey A. Hoffman [a], James W. Head [b]

[a] Department of Aeronautics and Astronautics, Massachusetts Institute of Technology, Cambridge, MA 02139, United States
[b] Department of Geological Sciences, Brown University, Providence, RI 02912, United States

ARTICLE INFO

Article history:
Received 8 November 2014
Received in revised form
5 March 2015
Accepted 9 March 2015
Available online 17 March 2015

Keywords:
Lunar surface exploration
Inflatable habitat
Environmental Control and Life Support System
Systems engineering
Lunar thermal modeling
Human space exploration

ABSTRACT

This paper presents the conceptual design and analysis of a system intended to increase the range, scientific capability, and safety of manned lunar surface exploration, requiring only a modest increase in capability over the Apollo mission designs. The system is intended to enable two astronauts, exploring with an unpressurized rover, to remove their space suits for an 8-h rest away from the lunar base and then conduct a second day of surface exploration before returning to base. This system is composed of an Environmental Control and Life Support System on the rover, an inflatable habitat, a solar shield and a solar power array. The proposed system doubles the distance reachable from the lunar base, thus increasing the area available for science and exploration by a factor of four. In addition to increasing mission capability, the proposed system also increases fault tolerance with an emergency inflatable structure and additional consumables to mitigate a wide range of suit or rover failures. The mass, volume, and power analyses of each subsystem are integrated to generate a total system mass of 124 kg and a volume of 594 L, both of which can be accommodated on the Apollo Lunar Roving Vehicle with minor improvements.

1. Introduction

The lunar surface exploration conducted during the Apollo missions remains one of the major accomplishments of NASA. The later Apollo missions demonstrated the value of vehicular surface exploration by increasing the range and scientific capabilities [1]. The total cost of the Apollo program was reported to Congress as 129 billion [2] (in 2010 US dollars). Considering that the Apollo program generated a total of 3 days and 6 h of lunar surface EVA time [3], an average of $1.7 billion dollars (2010) was spent per hour on the surface of the Moon. Although this is an oversimplification of the amortization of Apollo program costs, it provides an order of magnitude estimate for the cost of lunar surface exploration.

Improving surface exploration technology to increase science capability can add significant value to lunar exploration. For example, doubling the distance that astronauts can range from the lunar base opens up a host of new scientific objectives compared to Apollo capabilities. This is particularly true due to the immense amount of basic information obtained from the Apollo and Luna samples, combined with the orbital remote sensing data that has been obtained since the Apollo Era. The central peaks of the 96 km diameter Copernicus impact crater were seriously considered as a landing site for the later Apollo missions due to the importance of Copernicus in understanding the chronology and geological history of the Moon. The logic was to sample the solidified impact melt on the floor of the crater to obtain an absolute age of the cratering event. The central peaks

* Corresponding author. Tel.: +1 651 485 4539.
E-mail address: schr0910@umn.edu (S.S. Schreiner).

http://dx.doi.org/10.1016/j.actaastro.2015.03.012
0094-5765/

themselves were also thought to uplift deeper crustal material, but its mineralogy and composition were poorly known. These two major objectives could be accomplished by landing several kilometers from the peaks and using the Lunar Roving Vehicle to access the peaks. Since this time, high spatial and spectral remote sensing data [4] have revealed: (1) an amazing array of mineralogy on the floor and peaks, (2) a diversity in the impact melt deposit characteristics and mineralogy, and (3) abundant evidence of specific windows (craters, cracks, pits) into these units.

The nature and diversity of these units promises a much greater science return if they can be accessed. Increasing the traverse radius from the lunar base by a factor of two would bring virtually all of these features into the range of access and detailed analysis. The identification of minerals in specific outcrops [4] means that the increased EVA range can be optimized by careful traverse planning. Increased stay time and capability to return more sample mass would further optimize the scientific harvest from targets such as Copernicus.

As humanity looks to return to the Moon in a more sustained manner, lunar surface exploration systems will need to evolve from a system designed for short-term sorties to a more flexible system capable of exploring broader areas for longer durations. The conceptual design presented in this paper is set within the context of the next generation of lunar exploration. The earliest future lunar missions are assumed to be comparable in capability and scope to the late Apollo missions. Rather than the large pressurized roving vehicles and permanent base envisioned under the Constellation program [5,6], this paper assumes sortie missions with a modest increase in landing mass and surface duration compared to the late Apollo missions. In contrast to previous lunar habitat designs, for instance the Lunar Stay Time Extension Module [7], this system is designed to dramatically increase scientific capabilities with a modest increase in Apollo program designs.

The late Apollo missions utilized one Lunar Roving Vehicle, which constrained roving missions to stay within the walk-back distance from the Lunar Module (LM) to ensure that if the rover broke the astronauts could walk back to the LM. It is assumed that early future missions will have two rovers on the lunar surface and a crew of three or four. This will allow removal of the walk-back constraint, dramatically increasing the reachable exploration area. Within the context of this mission architecture, this paper presents a conceptual design that could be incorporated onto a variety of rover designs to dramatically increase mission capability and safety with a modest increase in rover capabilities.

The system presented in this paper is designed to support a two-day exploration mission away from the lunar base. As shown in Fig. 1, this system is composed of an inflatable habitat, an Environmental Control and Life Support System (ECLSS) on the lunar rover, a solar shield and a roll-out solar power array.

The system would be used as follows. After conducting a nominal day of surface exploration using the rover, the two astronauts would deploy the inflatable habitat, connect the rover ECLSS to the habitat, set up the solar shield over the habitat and deploy the solar array. The astronauts could conduct further scientific activities near that location if necessary. Instead of returning to base, the astronauts would then enter the habitat, doff their suits, and prepare for a second day of lunar exploration (eat, sleep, hygiene, etc.).

The rover ECLSS connects to the habitat via umbilical cables to maintain the atmosphere in the habitat. A thermal control unit on the rover is connected to the liquid cooling garments worn by the astronauts to provide active thermal control, while a solar shield is used to provide passive thermal control to minimize the load on the thermal control unit. The ECLSS contains a carbon dioxide scrubber, a "slurper" to remove humidity, an oxygen tank for respiration, and a water tank for the sublimator, crew hydration, food preparation, hygiene or medical use. The solar array provides power for the overnight system and recharges the rover batteries for the second day of exploration.

The work presented herein also assessed the feasibility of integrating the proposed system into a lunar rover. The Apollo Lunar Roving Vehicle (LRV) was used as a baseline design, although other rover designs could certainly be used as well. Fig. 2 depicts the operational system stowed on the

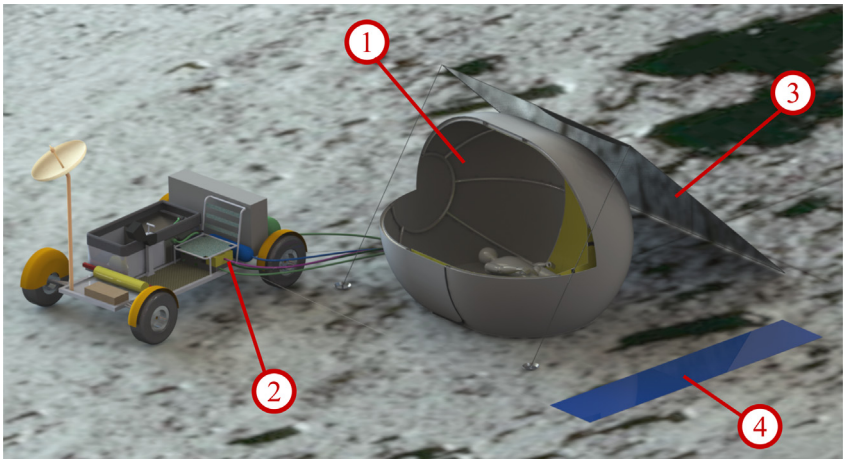

Fig. 1. A cutaway view of the operational system in its deployed state. The inflatable habitat (1) provides an overnight shelter in which two astronauts can sleep, while the Environmental Control and Life Support System on the rover (2) maintains the habitat internal environment. The thermal shield (3) mitigates solar radiation, and a solar array (4) supplies power.

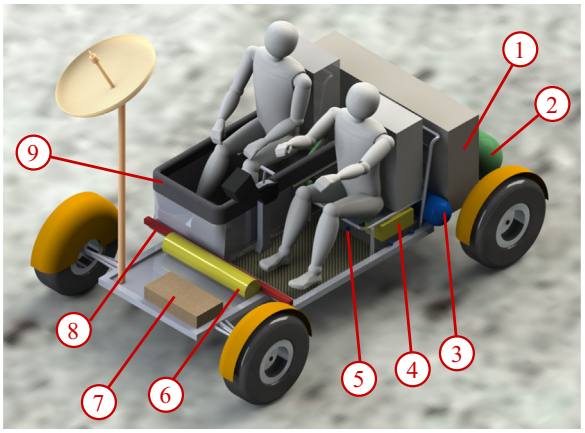

Fig. 2. The Apollo Lunar Roving Vehicle fitted with the stowed inflatable habitat (1), O_2 tank (2), H_2O tank (3), sublimator (4), CO_2 scrubber (5), stowed solar array blanket (6), folded thermal shield (7), thermal shield structural poles (8), emergency inflatable shelter (9).

LRV to demonstrate the feasibility of incorporating it into a rover design. This figure depicts the stowed inflatable habitat, oxygen tank, water tank, sublimator, CO_2 scrubbing system, solar array rolled into a cylindrical container, solar shield folded into a box, structural poles for the solar shield, and a small, one-person emergency inflatable shelter.

The emergency inflatable shelter was included to provide fault tolerance in the face of suit or rover failures. Although the inflatable habitat can be utilized to address a small range of emergency scenarios, scenarios involving rapidly deteriorating suit functionality necessitate a separate emergency inflatable that can be quickly deployed. The separate emergency inflatable can be quickly deployed around the passenger seat and sealed using an airtight zipper. A reserve oxygen tank and a CO_2 scrubber are connected to the internal volume of the emergency inflatable to provide a breathable atmosphere. The astronaut with the damaged suit can then sit in the emergency inflatable while the second astronaut drives the rover back to the base. The inflatable can then be detached from the rover and carried into the base's airlock if the suit damage is serious enough to warrant such action. The additional consumables included in the emergency system can also be used to support both astronauts in the case of a rover failure while they either repair the rover or await rescue.

Section 2 presents the inflatable habitat design, with an emphasis on structural validation, geometric optimization and a novel flexible membrane airlock concept. The design of a solar shield and thermal control unit, with a focus on the thermal modeling of the lunar environment, inflatable habitat, and solar shield, is discussed in Section 3. Section 4 gives an overview of the Environmental Control and Life Support System. Section 5 presents the design and sizing of the solar power array. In Section 6, the integration of the subsystem sizing models is presented to provide estimates of the total system mass and volume.

2. Inflatable habitat

To enable an overnight stay, the astronauts will require a pressurized environment in which they can remove their suits and sleep. The temporary habitat must be lightweight, portable, have a low mass and a high deployed-to-stowed volume ratio, which naturally leads to an inflatable design. This section presents the conceptual development and structural analysis of the inflatable rib support structure, optimization of the inflatable geometry, and suggested packaging of the inflatable structure.

2.1. Inflatable ribbing concept

When the astronauts first enter the inflatable habitat, the airlock volume requires a support structure in order to retain its internal shape while at zero internal pressure. Inflatable ribbing may be chosen for structural support. This ribbing consists of a frame of small-diameter inflatable tubes that, when inflated to high pressure, provide a rigid structure for the habitat. Thus, the astronauts can inflate the ribbing prior to entry without filling the interior of the habitat with O_2. Then the astronauts can enter the habitat, close the airlock, and fill the interior of the habitat to the desired pressure. A similar inflatable ribbing concept is used in commercially available inflatable camping tents.

2.2. Flexible membrane airlock design

To reduce the total size of the habitat, a novel flexible membrane was designed such that the same internal volume could function as both an airlock and habitat. As shown in Fig. 3, a thin, flexible, airtight membrane divides the internal habitat volume into an airlock side (left) and a habitat side (right). The membrane material is similar to the habitat outer surface without the micrometeorite protection, resulting in approximately 1/4 the surface density. The membrane is sized such that at any given time the entire volume can be used either as an airlock or as a habitat.

The concept of operations for entering the habitat using the flexible membrane airlock is illustrated in Fig. 3. After the astronauts have entered the habitat and pressurized the airlock, they remove their suits on the airlock side (top row of Fig. 3). Next, the airlock membrane is moved manually by the astronauts to its neutral transition configuration (middle row of Fig. 3). A valve in the membrane is used to regulate air flow from one side of the habitat to the other while the membrane is moved and the flow path is filtered to ensure that lunar dust is not transferred from the airlock side to the habitat side. After moving the membrane to the neutral position (in which it divides the habitat into two equal halves), the astronauts unzip an airtight zipper and proceed to the habitat side through the hole in the airlock membrane. Equipment is passed through in the same way. Next, the airtight zipper is closed and the membrane is manually moved towards the airlock side, maximizing the volume of the habitat side (bottom row in Fig. 3). The astronauts close the valve to the airlock side and then conduct activities within the habitat.

Although the air filter will mitigate dust transport to the habitat volume, removing dust attracted to the astronauts' bodies is an issue that warrants further investigation. Modeling dust transport and the effectiveness of removal mechanisms was deemed beyond the scope of this work, but it is likely that whatever technology chosen

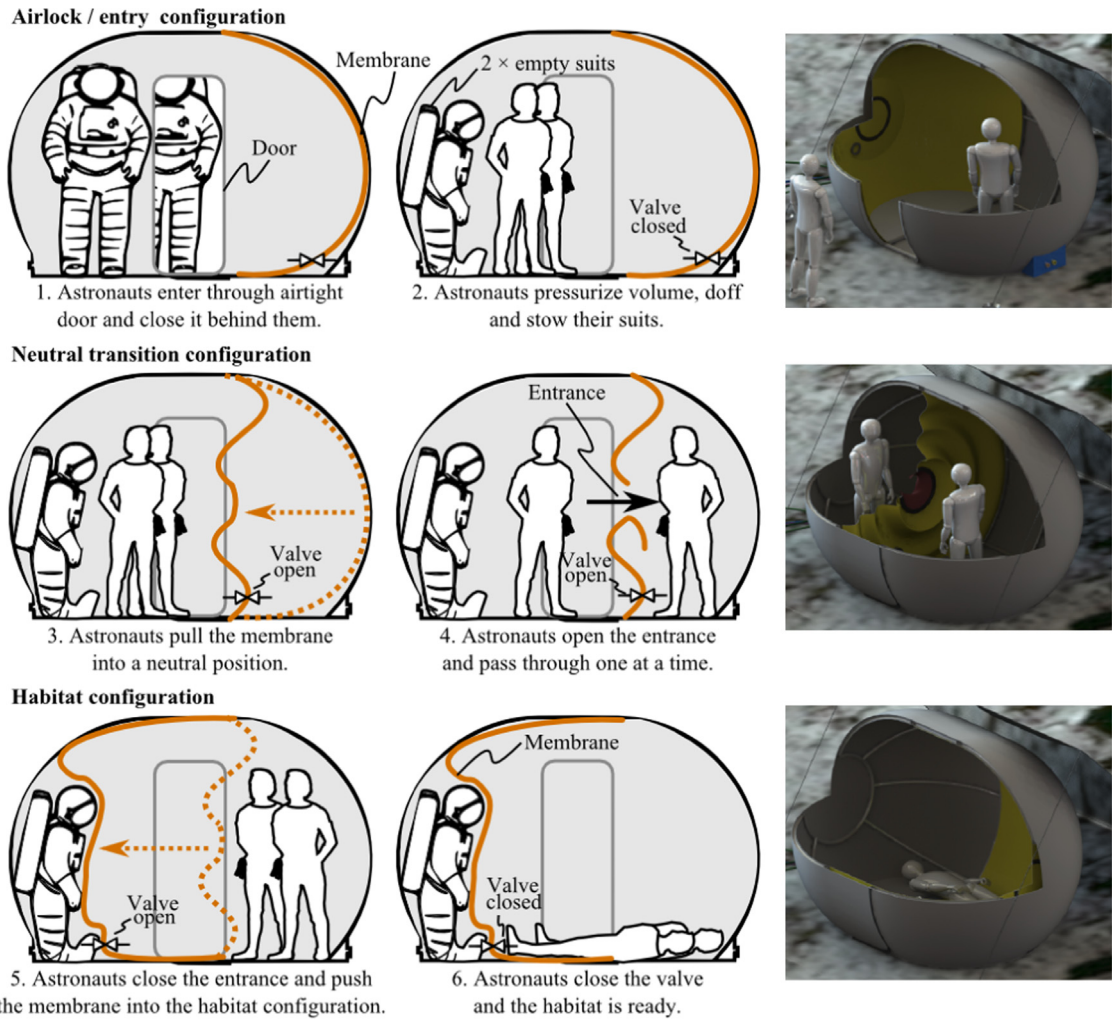

Fig. 3. The concept of operations for entering the habitat with inflatable ribs and the flexible membrane airlock. This novel concept allows the internal volume to be used as both an airlock and a habitat.

to remove dust at the lunar base can also be used in the inflatable habitat – including pressure vacuums, magnetic wands, and other preventative measures [8].

When considering entry and exit of the habitat, a net could potentially be used to restrain the airlock membrane in its neutral transition position in circumstances where the habitat side is pressurized but the airlock side is not. With a net in place, only partial venting of the volume would be required for entry and exit. The flexible membrane concept makes efficient use of the available space and reduces the total required internal volume of the habitat.

2.3. Inflatable geometry optimization

A preliminary geometric analysis was used to select a cylindrical geometry with hemisphere end caps and a flat floor. The cylinder was designed to accommodate the two astronauts standing vertically to don/doff their suits and the two astronauts sleeping side-by-side. The design was further constrained to a minimum interior volume of 12 m^3 as a conservative estimate [9], and was required to have a flat cylinder wall between the end caps that was long enough to accommodate a door 0.75 m wide for entry and egress. The radius of the cylinder, the width of the flat floor, and the length of the cylinder were optimized to ensure that these requirements were met while minimizing the total mass of the inflatable skin and ribbing. The optimized pill design was found to result in a significantly lower mass when compared to the baseline sphere geometry, with mass savings on the order of 10–20 kg (25–50%).

Fig. 4 shows a CAD model of the optimized flat-floor cylinder geometry. Table 1 gives the mass and volume of each component in the inflatable subsystem and Table 2 gives the dimensions of the optimized geometry. The material thicknesses were estimated based on the materials used in the Apollo suits [10] and the densities of the materials composing each layer. Typical packing factors (packaged volume divided by material volume) for space inflatables with little to no hardware are in the range of 1.25–2 [11]. As a conservative estimate, a packing factor of 2 was used to estimate the total packed volume.

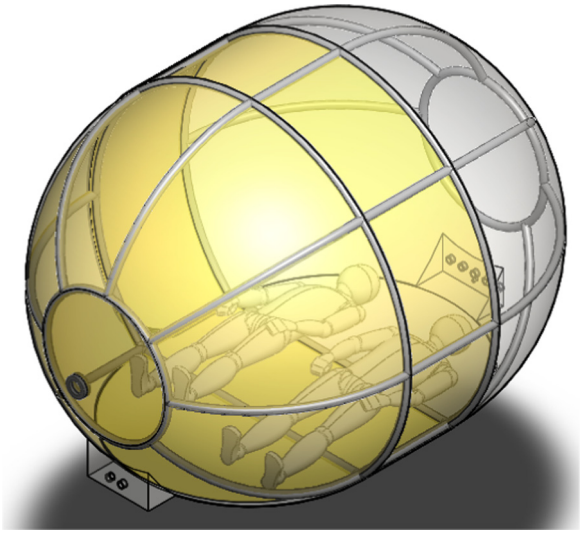

Fig. 4. The inflatable design with the optimized geometry that minimized mass and packing volume while satisfying minimum human living space requirements.

Table 1
Optimal inflatable pill mass and volume.

Component	Mass (kg)	Thickness (mm)	Material volume (m^3)
Support ribbing	1.10	0.09	0.0007
Adjustable airlock	4.04	1	0.0160
Wall/ceiling	26.27	5	0.1117
Floor	3.60	4	0.0155
Total	35.01	–	0.1440
Packed volume	–	–	0.2879

2.4. Inflatable structural analysis

A structural analysis was carried out on the inflatable to ensure it could support the various loading requirements. Here, the bending moment of a basic beam element determines, to a large extent, the load bearing ability of the structure. An inflatable beam member with circular cross section was chosen because of its inherent lack of stress concentrations when pressurized. The limits of strength of an inflated cylindrical tube can be calculated by investigating the axial stress in the skin. Specifically, for a thin-walled axial member, an analytical expression for the maximum bending stress σ_{bend} can be derived and simplified by noting that $t \ll r$:

$$\sigma_{bend} = \frac{Mr}{I_{xx}} \tag{1}$$

$$I_{xx} = \frac{\pi}{4}\left(r^4 - (r-t)^4\right) \approx \pi r^3 t \tag{2}$$

where M is the bending moment, r is the rib radius, I_{xx} is the moment of inertia about the neutral axis, and the higher order terms of t are neglected in the approximation [12]. Since an inflatable rib material, which is fabric-like, can only withstand tension forces, the beam will fail when $\sigma_{axial} \leq 0$,

Table 2
The optimized geometry of the inflatable cylindrical flat-floor habitat.

Optimized geometry	
Cylinder radius	1.29 m
Cylinder flat side length	0.75 m
Maximum floor width	1.80 m
Maximum floor length	2.55 m
Maximum height	2.21 m
Interior volume	12.00 m^3
Door height	1.84 m

which occurs at the critical bending moment M_{crit} [12]:

$$M_{crit} = \frac{\pi}{2} p r^3 \tag{3}$$

where p is the internal pressure of the ribs. For the analysis herein, a critical bending moment $M_{crit} = 20$ N m was chosen and rib radius r and rib pressure p were traded off with one another. A safety factor SF = 1.5 was applied, meaning that the ribs are designed to accommodate as much as 30 N m of bending in the worst case. For smaller radii, larger pressures are required to support the same bending moment. A rib radius of 2.5 cm was chosen to constrain the design. At this radius, the required pressure is 1.2 MPa, which is achievable by the upstream O_2 tank if at a pressure of 6.2 MPa. The resultant axial force that a single beam can support is 2400 N, or 1480 kg under lunar gravity. Since this is far in excess of any expected axial load, bending characteristics are used below to determine structural limits.

Silicone-coated Vectran was selected as the rib material for its high strength-to-weight ratio, temperature stability, and flight heritage. Vectran is a melt-spun liquid crystal polymer with excellent thermal stability, low creep, high strength, and chemical stability [13]; the Silicone coating ensures that the material is airtight. An identical material was used for the landing airbags of both the Mars Pathfinder and Mars Exploration Rover (MER) [14]. The material properties of the Silicone-coated Vectran used for the airbag bladder and restraint material in the MER missions, shown in Table 3, along with the pressure p and rib radius r specified above, are used to obtain a safety factor of 2.78 for skin stress. This increased safety factor allows some margin for the air used to inflate the ribs to expand due to temperature fluctuations.

To validate the rib structure's ability to support the inflatable under lunar gravity, an equivalent aluminum structure was generated for the purposes of conducting a finite element analysis (FEA) study. The equivalent aluminum 6061-T6 beam was obtained by determining the radius r_e of a cylindrical beam that yields at the same bending moment as the designed inflatable rib member. For the critical load considered above, and the yield stress of aluminum 6061-T6 ($\sigma_{e_{max}} = 275$ MPa), the equivalent beam radius was $r_e = 5.18$ mm. The FEA study was run in SolidWorks Simulation on an equivalent structure to ascertain whether it would yield under the combined weight of the ribs, the air in the ribs, the airlock, and outer shell of the habitat. Note that only the stresses, and not the displacements or strains, can be used from this study, since elastic modulus of the inflatable

Table 3
Properties of the Silicone-coated Vectran used on the Mars Exploration Rovers' airbags [14] and the inflatable ribs of the habitat.

Vectran layer	
Yarn	200 dernier Vectran HS
Weave	50 × 50 plain weave
Area density	0.092 kg/m^2
Linear ultimate tensile strength	84 940 N/m
Estimated thickness[a]	0.065 mm
Silicone layer	
Area density	0.054 kg/m^2
Estimated thickness[a]	0.024 mm

[a] The thickness was estimated by dividing the real density by the material density, but is not explicitly stated in [14].

beams was not considered. The results indicated that the rib structure is able to support itself, the air in the ribs, and the airlock and outer shell of the habitat without yielding. A large safety factor of approximately 10 is present, indicating that the structure could be used as an additional support for hanging equipment. The internal pressure on the outer shell of the habitat will provide additional supporting force; this is not considered herein, since the most structurally demanding case for the ribs will be supporting the habitat when it is unpressurized.

2.5. Inflatable deployment and stowing

The inflatable habitat will be folded and packaged into a manageable volume to fit on the rover. To deploy the habitat, the astronauts will remove the habitat from its container and unfold it on a flat surface. The ribs will then be inflated, establishing the habitat structure. The astronauts can then enter the habitat according to the concept of operations detailed in Section 2.2.

To stow the habitat, after venting the internal atmosphere the astronauts will depressurize the inflatable ribbing and fold the habitat on the lunar surface. The folding of inflatables into small volumes is complex and has roots as varied as the parachute industry and origami [11]. To fit the packaged inflatable habitat on the rover, base dimensions were taken from the trunk of the Apollo Lunar Roving Vehicle: 1.4 m × 0.7 m [1]. Using the packaged volume of 0.2879 m^3 determined in Section 2.3 (packing factor of 2), the folded inflatable can be expected to fit into a rectangular prism of dimensions 1.4 m × 0.7 m × 0.294 m. Magnetic wands can perhaps be used to remove dust from the habitat prior to stowing it on the rover, though this operation may be more adequately performed at the lunar base.

3. Thermal management system

3.1. Thermal system overview

The deployed habitat will be subject to significant variation in net heat load due to fluctuations in human activity and the changing thermal environment throughout the lunar day. The high surface temperatures and sunlight during the lunar day may lead one to assume that a thermal regulation system will require only active heat rejection. However, the complex geometry of the deployed habitat with a solar shield, shaded regolith, and sunlit regolith creates the need for both heat rejection and heat generation, depending upon the time of the mission in the lunar day, which lasts ~14 Earth days [15]. Section 3.2 describes the heat transfer models developed to characterize the complex thermal environment of the deployed overnight habitat on the lunar surface.

To provide thermal stability within the habitat in the face of this complex thermal environment, two systems were incorporated into the design. The first system is a reflective solar shield designed to mitigate solar radiation and shade the regolith in the vicinity of the habitat. The solar shield was designed such that the shield area could be adjusted on the lunar surface to create appropriately sized regions of shaded and sunlit regolith. By controlling the geometry of the relatively "hot" and "cold" regolith regions and reflecting the majority of the incident solar radiation, the solar shield minimizes the heat rejection and generation requirements on the habitat. The second system is a thermal control unit (TCU) composed of a sublimator/evaporator[1] and heater on the lunar rover connected to the liquid cooling garments worn by the astronauts in the habitat. The TCU provides active thermal control to supplement the solar shield. These two systems are further described in Section 3.3.

3.2. Thermal model development

To design the solar shield and the thermal control unit, a thermal model of the habitat's external and internal environments was developed. This model accounted for heat loads on the habitat from external radiation sources as well as from the astronauts, the ECLSS, and electronics. Fig. 5 illustrates the exterior heat flows between the habitat, regolith (sunlit and shaded separately), and up to two solar shield panels layered on top of one another. The exterior model accounted for 35 different heat flows, but only 13 heat flows are shown in Fig. 5 for clarity.

The solar shield was designed as 2mil Kapton-E with a 50 nm Cr_3Si coating on one side and a 100 nm aluminum-oxide coating on the other. The relevant optical properties of lunar regolith and the habitat were taken from the Lunar Sourcebook [15] and existing NASA suit materials [16].

Radiative heat transfer ($Q_{n\to m}$) due to emission from body n to body m was modeled as

$$Q_{n\to m} = \alpha_m \epsilon_n \sigma A_n F_{n\to m} T_n^4 \tag{4}$$

where T_n, ϵ_n, and A_n are the temperature, emissivity, and surface area of body n, α_m is the absorptivity of body m, σ is the Stefan–Boltzmann constant, and $F_{n\to m}$ is the view factor describing the fraction of the emitted radiation from body n that is incident upon body m [17]. The view factors between all of the bodies in the thermal model were calculated using preexisting view factors for known

[1] A sublimator was modeled as part of the Thermal Control System. Future missions may consider utilizing evaporators for their increased robustness to contaminants, but this is unlikely to significantly increase the predicted thermal control unit mass or water usage.

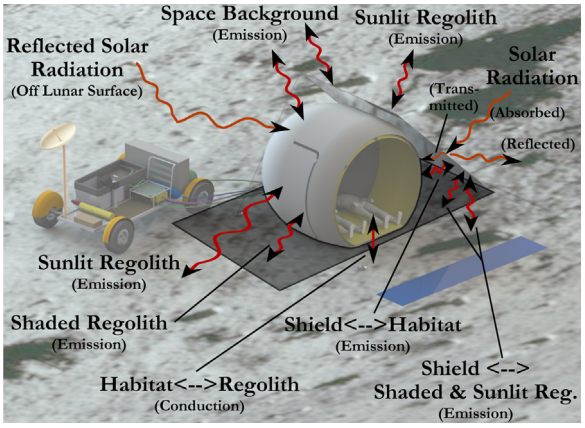

Fig. 5. The primary heat flows in the habitat thermal model, including radiative emission, reflection, transmission, and absorption between the habitat, the shaded and sunlit regolith, space, the sun, and the thermal shield.

geometries [18]. The incident solar flux was taken to be 1370 W/m^2 [19].

A major driver in the thermal model was the temperature of the sunlit and shaded regolith surfaces. To accurately model the regolith surface temperature, a 1D model simulation was developed after Henderson et al. [20], using data from Apollo 15 core measurements [21], to predict the surface temperature of the sunlit and shaded regolith regions. The model accounted for thermal momentum and Christiansen feature effects near the regolith surface to predict the temperature gradient after the setup of the habitat and solar shield. The results were validated against data from the Diviner instrument on the Lunar Reconnaissance Orbiter [22]. In effect, the transient surface model captured the dramatic rise in lunar surface temperatures due to incident solar radiation as well as radiation from the habitat itself.

The radiative flows, $Q_{n\to m}$, as well as reflection, transmission, and absorption terms were summed together for each body. Solving for the steady-state solution for the system $\left(\sum_n Q_{n\to m}=0\right)$ provided a means to calculate the net heat flow to the habitat.

The thermal model also accounted for heat generated by the electronics and the two astronauts within the habitat, the exothermic CO_2 scrubbing reaction, as well as the heat rejected or generated by the thermal control unit. The heat generated by two astronauts inside the habitat was taken to be 176 W while sleeping and 278 W while awake [23]. From the power analysis presented in Section 5, the heat generated by the electronics in the habitat was estimated to be 40 W.

Although the thermal model described thus far was used to find the steady state thermal equilibrium of the habitat, it was necessary to develop a second thermal model of the internal habitat atmosphere. A high heat load on the habitat will be conveyed through the interior atmosphere before being transported by the liquid cooling garments and rejected by the thermal control unit on the rover. If the magnitude of this heat flow is high enough, it can result in unsuitable atmospheric temperatures.

To capture this effect and ensure appropriate atmospheric temperatures, the second thermal model was developed to study atmospheric temperature as a function of the heat transfer from the habitat shell to the liquid cooling garment via the habitat atmosphere. This model accounts for conduction, radiation, and convection between the astronauts, habitat shell, and atmosphere, as well as the latent heat from the astronauts' breath. The surface area of the liquid cooling garment (LCG) was taken to be 2.0 square meters or approximately equal to the surface area of human skin [24]. As one would expect, at room temperatures convection dominates the heat transfer between the atmosphere and the LCG.

The interior atmospheric thermal model find the steady state solution by balancing the heat flow between the habitat shell and the atmosphere with the heat flow between the atmosphere and the LCG. By setting these two heat flows equal to one another, the average air temperature can be approximated by considering the dominate convective heat transfer terms. Using the convective heat flow equation [17] and some algebraic manipulation, the average air temperature can be derived as a function of heat flow through the atmosphere:

$$T_a \approx Q_a\left(\frac{1}{hA_g}\right)\left(\frac{A_h+A_g}{A_h-A_g}\right)-T_g \tag{5}$$

where Q_a is the heat flow through the atmosphere, h is the heat transfer coefficient, A_g and A_h are the area of the garment and the area of the habitat shell and T_g, T_a, T_h are the average temperatures of the garment, air and habitat respectively.

Fig. 6 displays the air temperature (T_a) from Eq. (5) as a function of the net heat load passing through the habitat to the LCG (Q_a). The two dashed horizontal lines depict the bounds on the control range of the Space Shuttle [23], which were taken as reasonable limits for the thermal model. The diagonal solid line shows the steady state average atmospheric temperature while astronauts are sleeping. The figure shows that a larger heat flow from the habitat to the TCU results in higher atmospheric temperatures. Fig. 6 demonstrates that when the astronauts are sleeping on the ground of the habitat, a net heat flow within $\approx \pm 100$ W

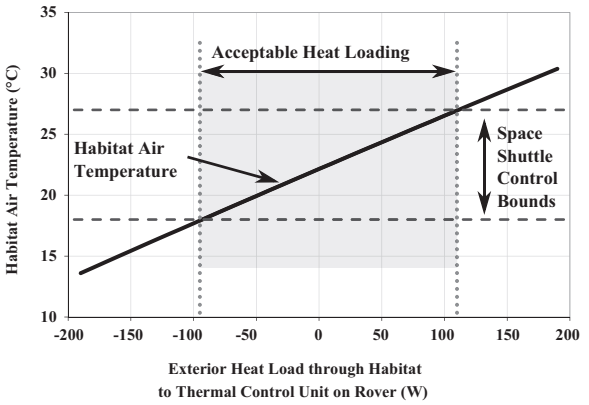

Fig. 6. Habitat internal air temperature as a function of net heat flow into the habitat, assuming that the liquid cooling garments are worn by both astronauts.

will result in a tolerable atmospheric temperature. When the astronauts are standing, a greater surface area of the LCG will be exposed to the air. This will increase the ability of the system to control air temperature at higher heat flows beyond the nominal range of $\approx \pm 100$ W. It should be noted that these bounds are conservative, because the model assumes that the outer and inner layer of the habitat shell are at the same temperature. In reality, insulation through this layer will result in an internal habitat shell temperature and air temperature that are closer to the temperature of the LCG than the current model predicts.

3.3. Thermal system design

The thermal models described above were used to calculate the net heat load to the habitat as a function of the solar shield and thermal control unit designs. The external radiation model described in the preceding section was primarily used to design the geometry, reflectivity, and emissivity of the solar shield such that it could minimize the requirement for active thermal control across the broadest possible range of solar angles, rather than limiting the mission to a small time range during the lunar day. To achieve this versatility, two degrees of freedom in the geometry of the solar shield were employed: deployment factor and orientation.

The *deployment factor* is the ratio of shield length (in the East–West direction) to the diameter of the inflatable habitat. Deployment factors larger than 1.0 provide shade to both the habitat and the surrounding surface regolith. This ratio was limited to a maximum of 2.25 and a minimum of 1.0 due to a breakdown in model accuracy when the shield is smaller than the cross-sectional area of the habitat. The thermal analysis revealed that the surface temperature and geometry of the shaded and sunlit regolith were large drivers in the net radiative heat flow to the habitat. The exterior thermal model had to capture these effects for a given solar shield geometry and sun angle. By varying the deployment ratio, the net heat load to the habitat could be passively controlled.

The second degree of freedom, *orientation*, refers to the direction that the reflective side of the shield faces. The shield was designed to be highly reflective on one side and highly absorptive on the other. To mitigate high heat loads on the habitat, the shield can be oriented with the reflective side up to reject the majority of the incident solar radiation. In scenarios where the habitat needs to be actively heated, the shield can be oriented with the absorptive side up to absorb solar radiation and re-emit it towards the habitat. Furthermore, with the reflective side pointed towards the habitat, the radiation emitted from the habitat is primarily reflected back to the habitat rather than transmitted to deep space.

A depiction of the shield at two different solar angles is shown in Fig. 7. The top graphic illustrates a deployment ratio of 2.25 with the reflective side facing up and the bottom graphic shows a deployment ratio of 1.56 with the reflective side facing down (towards the habitat).

With these two degrees of freedom, the solar shield can be adjusted on the lunar surface to the appropriate deployment ratio and orientation to minimize the net heat flow to the habitat. Fig. 8 depicts the optimal shield orientation and deployment ratio that maintain an acceptable heat load, and therefore atmospheric temperature, in the habitat throughout the lunar day. The shield configurations shown in Fig. 7a and 7b correspond to times of 7.5 and 3.7 days after lunar dawn, respectively.

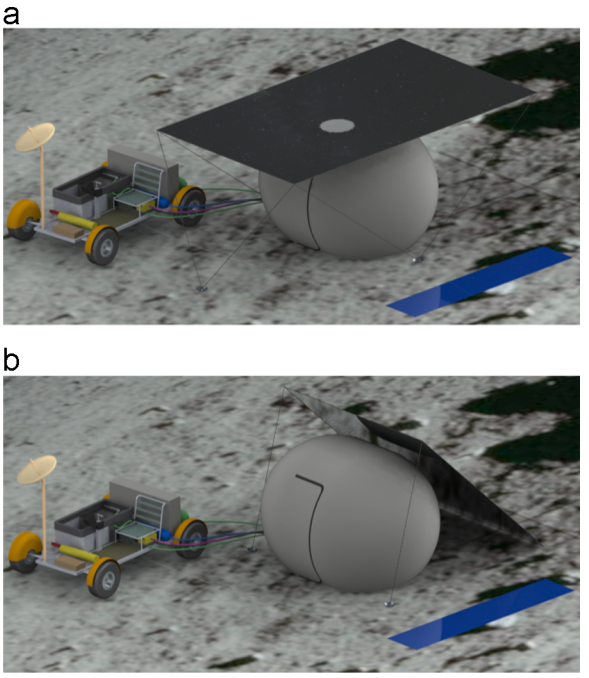

Fig. 7. Thermal shield configurations for two examples of angle, reflective side direction, and deployment ratio values considered in the model of the solar shield. (a) Shield deployed perpendicular to a solar angle of 90° above the horizon, with the reflective side pointing up. Deployment ratio of 2.25. (b) Shield deployed perpendicular to a solar angle of 45° above the horizon, with the reflective side pointing down. Deployment ratio of 1.56.

A number of conclusions can be drawn from Fig. 8. Up until 2 days after lunar dawn, the regolith is cold enough and the area of regolith shaded by the habitat is large enough (due to the oblique sun angle) that the shield cannot maintain a net heat load within the $\approx \pm 100$ W acceptable bounds, even when fully deployed with the highly reflective side facing the habitat. Around the second day after lunar dawn, the shield is able to maintain a close-to-zero net heat load with the highly reflective side pointed at the habitat and a deployment ratio of 2.25 (the maximum allowable value). For missions later in the lunar morning, when the regolith is at a higher temperature and the area of regolith shaded by the habitat is smaller (due to a sun angle closer to 90 degrees from the lunar surface), the deployment ratio can be decreased to maintain equilibrium by absorbing and reflecting less solar radiation to the habitat.

Fig. 8 shows that around 4.5 days after lunar sunrise, the deployment ratio would naturally continue below 1.0, meaning that the solar shield no longer covers the entire habitat. At this point, the radiative model developed herein cannot be used, as the radiation view factors no longer apply. Despite this, it is anticipated that further decreasing the deployment ratio of the solar shield below 1.0 will maintain

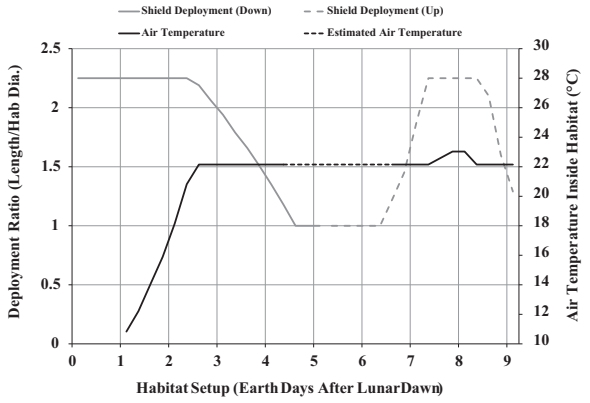

Fig. 8. The air temperature inside the habitat (right *y*-axis) from zero to nine Earth days after lunar dawn. The deployment ratio (left *y*-axis) and orientation of the solar shield, optimized for minimal thermal loading to the habitat.

a zero net heat flow. This is illustrated using the dotted black line in Fig. 8.

Around day 5, it becomes ideal to reverse the orientation of the shield such that the reflective side is pointed outward to reduce incident solar radiation. After this point, the deployment ratio would begin increasing throughout the lunar day to continue to maintain a net heat flow of zero. Although the deployment ratio reaches a maximum of 2.25 beginning around day 7.5, the total heat flow does not exceed ≈ 100 W at solar noon and the graph is then roughly symmetric across solar noon, with an offset for the thermal inertia of the regolith.

Using the bounds determined from Fig. 6, the suitable mission window starts around 2 Earth days after lunar dawn. The end of the suitable mission window was approximated to be around 12 Earth days after lunar dawn, using the symmetry observed in Fig. 8, though the thermal inertia of the lunar regolith will likely extend the suitable mission window beyond day 12.

Once the thermal shield design was validated using these models, the maximum shield area was used to generate an estimate of shield mass. Furthermore, a finite element analysis was conducted to design a lightweight structure to support the shield. The total estimated mass of the solar shield and its support structure is presented in Section 6.

Although the solar shield provided passive thermal management for a wide range of sun angles, it was deemed necessary to include an active thermal control system to regulate the habitat temperature in response to short-term fluctuations in heat load. This system, called the Thermal Control Unit (TCU), was composed of a sublimator/evaporator (see footnote 1) and heater on the lunar rover connected via umbilicals to the liquid cooling garments (LCG) worn by the astronauts in the habitat.

Using the solar shield design determined using the analysis described above, the maximum change in net heat load due to the changing sun angle and astronaut activity over a 12-h period was used to determine the maximum heat rejection and generation requirements on the TCU. This analysis was run for all times within the acceptable mission window to ensure that the TCU could provide adequate active thermal control over any given 12 h period. For missions involving more than 12 h within the habitat, the solar shield can be adjusted via a mechanical actuator controlled by the astronauts in the habitat.

To heat the water running through the LCG, a bypass valve in the LCG transport loop can be actuated to redirect water to bypass the sublimator/evaporator (see footnote 1) and instead flow to a heat exchanger which is exposed to direct sunlight. A diagram of this setup is included in the broader system schematic shown in Fig. 9. A thin copper pipe heater with flow length 1 m and side dimension 42 cm × 42 cm was designed to supply up to 250 W of heat.

The design of the sublimator housing and its components used the Apollo PLSS design [25] as a baseline and was then dynamically sized off the maximum heat loads using the equations found in [26]. The sublimator was sized such that the ice layer will not completely melt under the maximum heat load, which would cause a "blowby" effect of the feedwater through the porous plate. Taking this consideration into account, the sizing model calculates the area of the porous plate and the thickness of the ice layer, which were translated into sublimator dimensions. Approximately 15.2 cm of extra depth behind the porous plate was added to account for the LCG cooling fins, the water vent loop, and the bottom plenum [25]. In addition to system dimensions, the sublimator model calculates the mass flow rate of water to the environment, which was integrated over the mission timeline to determine the total amount of water needed to run the sublimator throughout the mission. Table 4 displays specifications of the sublimator that was designed to support two astronauts within the habitat for the duration of the overnight mission.

It should be noted that future missions may consider alternate means of heat rejection, such as evaporator units which are less sensitive than sublimators to contaminants in the feedwater. However, basing this analysis on proven technology provides an upper bound on mission mass while minimizing technology development requirements.

4. Environmental Control and Life Support Systems

To enable an overnight stay on the lunar surface, the system needs to provide a suitable environment and consumables such as water and food. To meet this need, an Environmental Control and Life Support System (ECLSS) was designed to support two astronauts during the overnight stay and to recharge the astronauts' Portable Life Support Systems (PLSS) for a second day of exploration. The demands of the first day were not included in the system design because they would be met by the astronauts' (PLSS).

To determine the appropriate ECLSS size, a human producer–consumer model was developed using data from NASA's Advanced Life Support Baseline Values and Assumptions Document [9] and Human Integration Design Handbook [23]. The different producer–consumer values for extravehicular activity (EVA), in-habitat awake, and in-habitat sleeping, were integrated with the mission timeline to calculate the required oxygen, water, and food, as well as

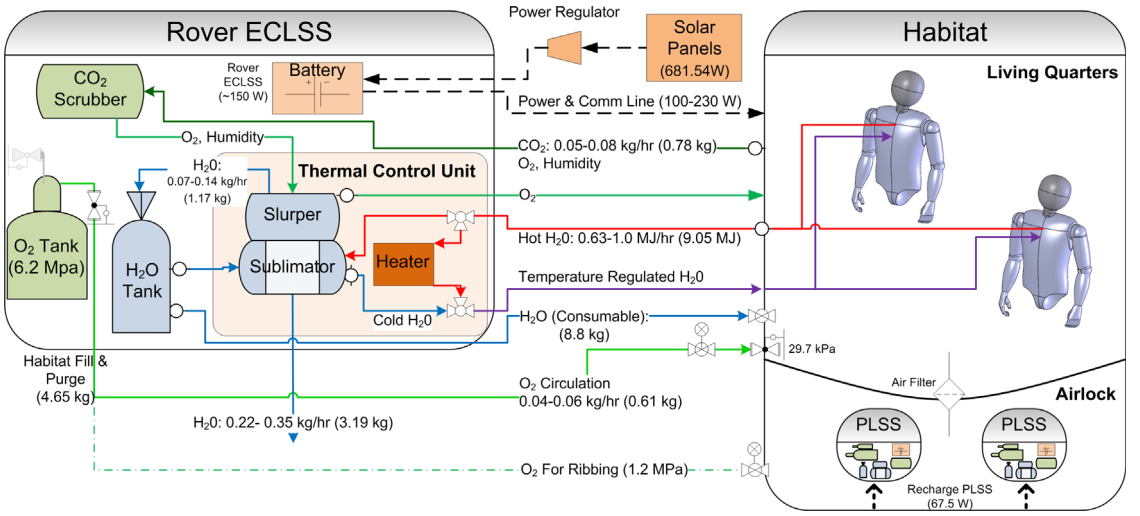

Fig. 9. A diagram of the interface connections between the Environmental Control and Life Support System (including the thermal control unit) on the rover with the habitat internal volume and astronaut liquid cooling garments.

Table 4
The sizing of the thermal control unit on the rover, designed to accommodate the maximum and minimum heat load on the habitat with two astronauts inside overnight.

Thermal control unit	
Sublimator system volume	6.0 L
Sublimator hardware mass	1.1 kg
Water required for sublimator	5.9 kg
Heater mass	1.6 kg
Water required for heater	0.05 kg

Table 5
Oxygen and water requirements and storage system sizing for the overnight mission.

Consumables storage	Oxygen	Water
Quantity required (kg)	8.1	23.9
Tank mass (kg)	6.8	4.0
Tank volume (L)	99.9	23.9

the required humidity removal and CO_2 scrubbing capability needed for the overnight mission.

The oxygen and water requirements for the mission were translated into tank sizes using the tank designs from the Space Shuttle EMU Handbook [27] as a baseline. In addition to the water required for human consumption, the water sublimated by the thermal control unit (discussed in Section 3.3) and the water to refill the suit sublimators for the second day of exploration were also included in the tank sizing. Table 5 displays the quantity of water and oxygen required to sustain the overnight mission.

The producer–consumer environmental model predicted the amount of CO_2 that the astronauts would produce through the mission timeline, which was then used to size the CO_2 scrubbing system. Three different CO_2 scrubbing technologies were considered: lithium hydroxide (LiOH), metal oxide (MetOx), and rapid cycle amine (RCA). Both LiOH and MetOx scrubbing cartridges have already been flown in the EMU suit [27], while RCA is currently under development. LiOH cartridges have the lowest mass, but are single-use only. MetOx cartridges can be regenerated using an oven at the base, but have a much higher mass. RCA cartridges weigh less than MetOx and more than LiOH, but they do not require replacement and thus reduce the number of cartridges needed. The total amount of CO_2 that needed to be scrubbed for the overnight mission was used to size the CO_2 scrubbing system for each of the three techniques. The results of this sizing are shown in Table 6.

The purpose of the scrubbing analysis was not to select a particular scrubbing technique, as whichever method is chosen for future lunar exploration suits will likely drive the scrubbing technique chosen for the overnight system. Rather, this analysis shows that, while all three techniques can meet mission needs, LiOH or RCA are somewhat preferable from the viewpoint of this system design.

Fig. 9 displays a comprehensive schematic of the interfaces between the ECLSS and thermal control unit on the rover and the inflatable habitat. Values of the calculated flow rates are shown where applicable, along with the total quantities required for the overnight mission concept in parenthesis.

5. Power system

The two day, overnight mission imposes a number of requirements on the power system. The system must supply power for a full day of operations, support the habitat and recharge the space suits overnight, and supply power for a second full day of operations before returning to base. The primary trade evaluated in the power system design was between a deployable solar array with rechargeable batteries and simply designing larger batteries to support the full mission. The power analysis revealed that including a solar array can save significant system mass compared to a larger battery design.

Table 6
The three options for the CO_2 scrubbing system sized for the two-day, overnight lunar surface mission. "Required No. of Cartridges" represents the total number of cartridges including the two that are originally in the two astronaut portable life support systems.

CO_2 scrubbing	Cartridge mass (kg)	Required no. of cartridges	System mass (kg)
LiOH	2.90	6	17.40
MetOx	14.52	6	87.12
RCA	7.26	4	29.04

To design the deployable solar array and rechargeable batteries on the lunar rover, a power model was developed to estimate the power demands and battery level throughout the mission. The power model includes the electric motors on the rover (locomotion), the ECLSS and thermal control unit on the rover, a communication system, a navigation system, power management, and science equipment, as summarized in Fig. 10. The battery level was calculated by integrating the net power load on the system over the mission timeline to generate a total energy requirement throughout the mission. Fig. 10 displays the estimated power load throughout the overnight two-day mission along with the resultant battery level.

The rechargeable batteries on the rover were chosen to be lithium-ion (Li-Ion) composites, due to their high energy density as well as their excellent discharge and wet life characteristics [19]. Furthermore, this design decision provides compatibility with the new human-rated extravehicular mobility unit (EMU) designs, which have also been designed to use Li-Ion composites [28]. The batteries used for this analysis were assumed to have energy densities of 320 W h/kg and 600 W h/L, respectively [29].

For the sake of redundancy and fault tolerance, the power system design utilized two batteries on the rover rather than one large battery. The concept of operations dictates that the solar array be deployed once the astronauts finish EVA activities on day 1, so the batteries were sized such that one was capable of supplying all of the power required up until that point in the mission with 20% capacity remaining. Table 7 displays the specifications of the battery sized for the two-day mission compared to a battery sized for a nominal one-day mission. The required increase in battery capacity is minimal, due to the fact that the batteries are recharged by the solar array after the first day of operations.

Portable, flexible roll-out solar arrays are commercially available and would be advantageous for lunar surface exploration missions [30]. It was assumed that the solar blanket would use Gallium–Arsenide (Ga–As) single-junction solar cells, which have a maximum efficiency of 18.5% [19]. It was also assumed that the solar blanket would have a conservatively high mass density of 2.5 kg/m^2 and array thickness of 5 mm [19], which allows extra margin for protection from radiation and the lunar environment, as well as for wiring and other supporting elements. The solar array was sized such that it could provide enough power to sustain the habitat overnight while also recharging the rover batteries and both space suit batteries, with an additional 10% safety margin added

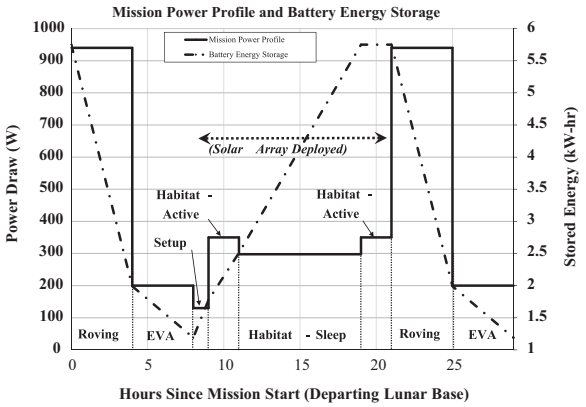

Fig. 10. The power profile (left axis, solid line) and stored energy of a single battery (right axis, dashed line) throughout the overnight two-day lunar surface mission.

Table 7
Power System comparison between a nominal single-day mission (Single Day) and the two-day overnight mission (Two Day).

Rover battery	Single day	Two day
Capacity (kW h)	10.3	11.5
Mass (kg) (10% *margin*)	35.4	39.5
Volume (L) (10% *margin*)	18.9	21.1
Solar array		
Array size (m^2)	–	2.8
Power output (W)	–	716.7
Array mass (kg)	–	7.1
Case mass (kg)	–	2.4
Array volume (L)	–	60.0

to the solar array area. A cylindrical, polyethylene storage case for the roll-out solar array was designed, using the Archimedian spiral equation to estimate the radius of the rolled-up array [31].

The two day, overnight mission power profile and energy level of a single battery throughout the mission are shown in Fig. 10, with the values for the power profile displayed on the left axis and the values for energy storage displayed on the right axis. Table 7 presents the predicted mass, volume, and other design parameters for the power subsystem required for the two day overnight mission compared to a nominal single day design.

The total power subsystem mass and volume, including batteries, solar array, and all accompanying components, were determined to be 49 kg and 89 L, respectively. Comparing this mass to the power system required for a nominal one day mission, we calculate that the extra mass incurred by adding the two day, overnight capability is approximately 13.2 kg.

The mass of the power subsystem with the solar array blanket was compared to the mass of an equivalent non-rechargeable power subsystem using batteries with a greater energy density (450 W h/kg), and it was found

that the rechargeable subsystem achieved mass savings of more than 30% over the non-rechargeable option.

6. Results: system mass and volume estimates

The subsystem designs described in the previous sections were integrated to generate an estimate of the mass, volume, and power for the entire system. The system boundary was drawn around the set of components that were required to provide the overnight stay capability on the lunar surface as well as a second day of lunar EVA. This means that the mass, volume, and power estimates are designed to give a sense for how much *additional* mass would need to be added to a lunar surface exploration system to enable the overnight stay capability.

Fig. 11 shows the mass breakdown for the system described in this paper. A further breakdown of the "ECLSS Consumables" slice is presented in the pie chart on the right of the figure. The primary drivers of system mass are the ECLSS, ECLSS consumables, and inflatable subsystems, which together compose approximately 3/4 of the entire system mass.

The mass of the proposed overnight system was estimated to be 124 kg. It should be noted that this estimate does not include any additional margin to account for the low Technology Readiness Level (TRL) of the design and the anticipated increase in mass with design maturation. An important conclusion is that the predicted mass of 124 kg is the same order of magnitude as the limited carrying capacity of the Apollo Lunar Roving Vehicle (~105 kg [1]). This indicates that the proposed operational system could fit on a rover with only a modest increase in carrying capacity compared to the Apollo LRV.

The volumetric breakdown for the system is shown in Fig. 12. This figure shows that the primary driver of system volume is the inflatable subsystem, which comprises almost half of the total system volume when stowed. The ECLSS also comprises a significant portion of the volume of the system, which can be primarily attributed to the large oxygen and water tanks required.

7. Conclusion

This work presents the conceptual design of a system to extend lunar surface exploration capabilities. As humanity looks to return to the Moon in a more sustained manner, extending surface EVA range and scientific capabilities can add significant value to a surface exploration program without the expense of large, pressurized rovers. The system designed for this purpose contains an ECLSS on the unpressurized rover, an inflatable habitat, a solar shield, and a solar power array. It will enable two astronauts to conduct a full day of lunar surface exploration, sleep and recover within the inflatable habitat at a location away from the lunar base and then conduct a second day of exploration before returning to the base. The proposed system has the potential to double the reachable distance from the lunar base, increasing the reachable area by a factor of four. Given that the Apollo missions reached a maximum distance of 4.7 miles away from the lunar lander [1], this system is expected to increase mission range to 9.4 miles as an extremely conservative estimate – due to the fact that this system also breaks the walk-back constraint on lunar surface exploration, it has the potential to enable mission ranges of over 12.5

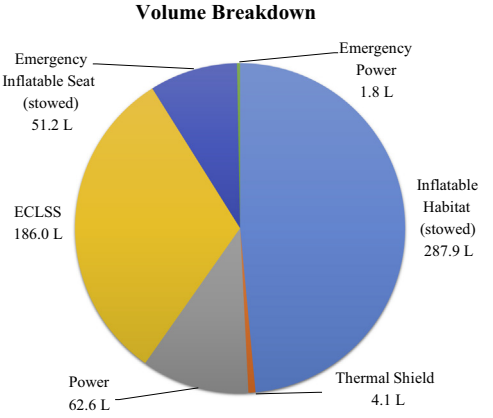

Fig. 12. The volumetric breakdown of the subsystems within the overnight system.

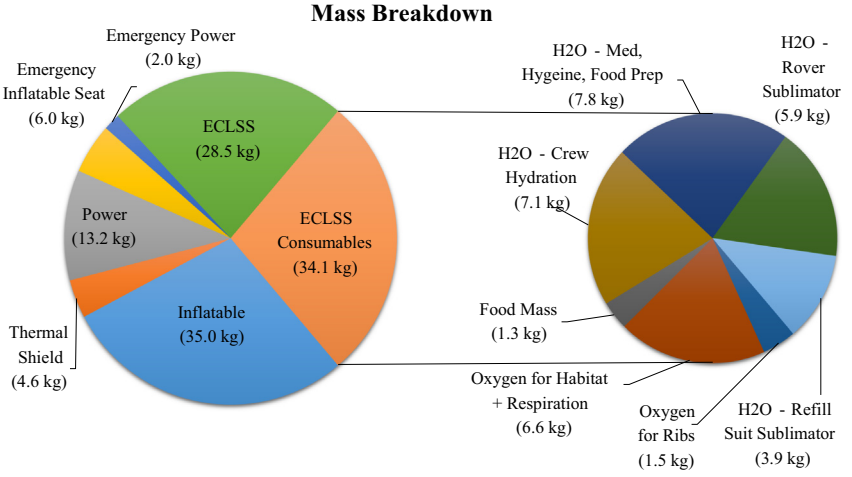

Fig. 11. The mass breakdown of the subsystems within the overnight system.

miles [1]. This increased mission range could enable single-outing missions to visit multiple locations to increase the scientific impact.

As exemplified by the mission to Copernicus central peaks [4], this increased capability would enable astronauts to address several fundamental scientific objectives, including (1) the age of Copernicus crater, (2) the chemical and mineralogical heterogeneity of impact melt, (3) modes of emplacement, differentiation and cooling of impact melt, (4) the mode of formation of central peaks, (5) the collapse and uplift of the floor of complex craters, (6) the origin and mode of emplacement of the mineral olivine, (7) the associations and origins of Mg-spinel, (8) the structure and composition of the deep crust in the central nearside of the Moon. The scientific return from other candidate landing sites would be similarly enhanced by these additional capabilities.

Additionally, because the proposed system contains an ECLSS and a single-person emergency inflatable, it adds a layer of fault-tolerance. In the event of a rover or suit failure, the astronauts can utilize these emergency capabilities to either wait for rescue or return to base. Thus, this system will further expand EVA capabilities by providing single-fault tolerance in the face of a wide variety of suit and rover failure modes.

The feasibility of the two day, overnight exploration system was evaluated and found to be attainable with a modest increase in capabilities compared to the Apollo Lunar Roving Vehicle. Assuming that future rovers have a marginally larger carrying capacity that the Apollo-era rovers, both the mass and volume of the proposed system can be accommodated by the rover to greatly increase the range and capability of science and exploration missions on the lunar surface. This mission-enabling technology provides a dramatic extension of lunar surface capabilities at such a modest increase in system design that it warrants further development and investigation.

Acknowledgments

The authors thank Dave Scott and Bruce Cameron for their guidance on the system design and project direction. The authors would also like to thank Aleksandra Stankovic for editing and proofreading the manuscript. The Open Access fee for this work was supported by NASA grant #NNX13AL76H.

References

[1] S.F. Morea, The lunar roving vehicle: Historical perspective, in: Lunar Bases and Space Activities of the 21st Century, vol. 1, 1992, pp. 619–632.
[2] U. States, 1974 NASA Authorization: Hearings, Ninety-third Congress, First Session, on h.r. 4567 (superseded by h.r. 7528), Print, 1974.
[3] R. Orloff, S. Garber, Apollo by the Numbers: A Statistical Reference, NASA, 2000.
[4] D. Dhingra, C. Pieters, J.W. Head, Copernicus crater: compelling science exploration target waiting for future missions, in: Annual Meeting of the Lunar Exploration Analysis Group, 2014.
[5] K. J. Kennedy, L. D. Toups, M. Rudisill, Constellation architecture team–lunar scenario 12.0 habitation overview, NASA Johnson Space Center, Rept. JSC-CN-19362, 2010.
[6] D. Akin, M. Bowden, A small pressurized rover concept for extended lunar and Mars exploration, in: Space 2005, 2005, p. 2005.
[7] C.I. Tynan, Jr., Lunar Stay Time Extension Module, NASA Technical Report.
[8] J.H. Agui, D.P. Stocker, NASA Lunar dust filtration and separations workshop report, Technical Report, NASA, 2009.
[9] N. Aeronautics, S. Administration, advanced life support baseline values and assumptions document (nasa/cr-2004-208941), 2004. URL ⟨http://ston.jsc.nasa.gov/collections/trs/_techrep/CR-2004-208941.pdf⟩.
[10] National Aeronautics and Space Administration, Space suit evolution: from custom tailored to off-the-rack, 1994 ⟨http://history.nasa.gov/spacesuits.pdf⟩.
[11] C. Jenkins, Gossamer Spacecraft: Membrane and Inflatable Structures Technology for Space Applications, vol. 191 American Institute of Aeronautics and Astronautics, Reston, VA, 2001. URL ⟨http://books.google.com/books?id=NZahLD6gXcoC⟩.
[12] L. Asheghian, J. Jacob, S.W. Smith, Innovative ground habitats for lunar operational outpost (igloo), in: 52nd AIAA/ASME/ASCE/AHS/ASC Structures, Structural Dynamics and Materials Conference 19th AIAA/ASME/AHS Adaptive Structures Conference 13t, 2011.
[13] Celanese Acetate LLC, Vectran Engineering Data, Technical Report. URL ⟨http://www.swicofil.com/vectranengineering.pdf⟩.
[14] J. Stein, C. Sandy, Recent developments in inflatable airbag impact attenuation systems for Mars exploration, AIAA 1900 (2003) 7–10. URL http://arc.aiaa.org/doi/pdf/10.2514/6.2003-1900.
[15] G.H. Heiken, D.T. Vaniman, B.M. French, Lunar Sourebook: A User's Guide to the Moon, Cambridge University Press, New York, NY, 1991.
[16] J.H. Henninger, Solar absorptance and thermal emittance of some common spacecraft thermal control coatings (reference publication 1121), Print, April 1984.
[17] Y.A. Çengel, A.J. Ghajar, Heat and Mass Transfer: Fundamentals & Applications, McGraw-Hill, New York, NY, 2011.
[18] J.R. Howell, A Catalog of Radiation Transfer Configuration Factors 3rd ed, 2010, ⟨http://www.thermalradiation.net/indexCat.html⟩.
[19] J.R. Wertz, D.F. Everett, J.J. Puschell, Space Mission Engineering: The New SMAD, Microcosm Press, El Segundo, CA, 2011.
[20] B.G. Henderson, B.M. Jakosky, Near-surface thermal gradients and mid-ir emission spectra: a new model including scattering and application to real data, J. Geophys. Res.: Planets 102 (E3) (1997) 6567–6580, http://dx.doi.org/10.1029/96JE03781.
[21] M.G. Langseth Jr., S.P. Clark Jr., J.L. Chute Jr., S.J. Keihm, A.E. Wechsler, The Apollo 15 lunar heat-flow measurement, Moon 4 (3–4) (1972) 390–410.
[22] D.A. Paige, B.T. Greenhagen, Diviner lunar radiometer experiment extended mission results: thermal, thermophysics, and compositional properties, in: 44th Lunar and Planetary Science Conference, vol. 44, 2013, pp. 2492–2492. URL ⟨http://www.lpi.usra.edu/meetings/lpsc2013/pdf/2492.pdf⟩.
[23] National Aeronautics and Space Administration, Human Integration Design Handbook (nasa/sp-2010-3407), January 2010 ⟨http://ston.jsc.nasa.gov/collections/_trs/techrep/CR-2004-208941.pdf⟩.
[24] J. Merchant, J. Kline, K.J. Donham, D.S. Bundy, C.J. Hodne, Human Health Effects, The University of Iowa, Iowa City, IA, 2002, 121–145 (Chapter 6.3). URL ⟨https://www.public-health.uiowa.edu/ehsrc/CAFOstudy/CAFO_6-3.pdf⟩.
[25] K. Thomas, Hamilton Sundstrand portable life support & space suit experience: Rev. d, December 2006.
[26] J.P. Shero, Porous plate sublimator analysis (Ph.D. thesis, Doctoral thesis), Rice University, 1970, http://hdl. handle.net/1911/14662. URL ⟨http://hdl.handle.net/1911/14662⟩.
[27] H. Sundstrand, NASA extravehicular mobility unit (emu) lss/ssadata book: Rev. h, December 2008.
[28] S.P. Russell, M.A. Elder, A.G. Williams, J. Dembeck, The Extravehicular Maneuvering Unit's New Long Life Battery and Lithium Ion Battery Charger, Technical Report, AIAA, 2010. URL ⟨http://ntrs.nasa.gov/archive/nasa/casi.ntrs.nasa.gov/20100030503.pdf⟩.
[29] M. Stout, Lithium-ion battery technologies with high energy density, accessed: 2014-07-03, May 2014. URL ⟨http://www.techbriefs.com/component/content/article/9-ntb/tech-briefs/physical-sciences/19567⟩.
[30] K.M. Trautz, P.P. Jenkins, R.J. Walters, D. Scheiman, R. Hoheisel, R. Tatavarti, R. Chan, H. Miyamoto, J.G. Adams, V.C. Elarde, et al., Mobile Solar Power, Technical Report, Naval Research Laboratory, 2012.
[31] H. Walser, P. Hilton, J. Pedersen, M.A. of America, Symmetry, MAA spectrum, Mathematical Association of America, 2000. URL ⟨http://books.google.com.br/books?id=rU8jvsJMKsgC⟩.